
**Guilhem Mollon[(1)], Vincent Richefeu[(1)], Pascal Villard[(1)], Dominique Daudon[(1)]**

# Assessment of Discrete Element Modelling parameters for rock mass propagation

**(1) UJF-Grenoble 1, Grenoble-INP, CNRS UMR 5521, 3SR Lab, Grenoble F-38041, France**

**Abstract** The efficiency of a numerical model depends on both the realism of the assumptions it is based on, and on the way its parameters are assessed. We propose a numerical model based on the discrete element method which makes possible, thanks to the definition of an appropriate contact law, to simulate the mechanisms of energy dissipations by friction and shocks during the propagation of an avalanche of granular material on a slope. The parameters of the contact model are obtained from laboratory experiments of single impacts. A particular attention was paid to the values of the run-out, the morphology of the deposit, the proportions of energy dissipations by impacts or friction, and the kinetic energies of translation and rotation. The results of this numerical study provide valuable information on the relevance of some usual assumptions of granular flow continuous models.

**Keywords** Discrete element method, rock avalanches, dissipative contact law, parameter identification, experimental validation

## Introduction

Understanding and prediction of rock avalanches are key elements for the risk management in the development of mountain areas. Due to the complexity of the involved mechanisms, numerical models such as continuous models (McDougal and Hungr [2004], Mangeney-Castelnau et al. [2003], Tommasi et al. [2008]) based on fluid mechanics or discrete element models (Cundall and Strack [1979]) are needed to estimate the morphology of the deposit or the propagation distance of a rock mass.

Compared with continuous models, discrete models allow more accurate modelling of the propagation phenomenon, without the need of accounting for all existing mechanisms of interaction. At the scale of an actual event, rather simple contact laws can be used without any loss of accuracy.

The model proposed here is based (i) on realistic block shapes and (ii) on the definition of simple interaction laws that hold physical parameters easily assessable. These laws incorporate the mechanisms of energy dissipation in a global way.

To validate this approach, which is extremely difficult to carry out in the case of rock avalanches, we replicated laboratory experiments conducted under idealized test conditions (Manzella and Labiouse [2009]). Model parameters, optimized through tests conducted on single brick release, were used to simulate the collective behavior of a set of bricks on a slope.

The advantage of the numerical model is that it gives access to quantities difficult to assess experimentally at any point of the granular mass: velocity and rotation of bodies, energy dissipated by friction or shocks with the slope or within the mass movement, nature of flow and geometry of the final deposit.

After the validation, the numerical model is used to evaluate the quality of some usual assumptions of continuous models of granular flows (i.e. assumptions of no-dilatancy and of velocity uniformity in a cross-section of the flow), and the relevance of some parameters by studying the different modes of energy dissipation along the slope and inside the flow.

## Numerical model

Discrete models have the advantage to model the deterministic movements of a set of interacting particles. We present in this section the numerical model implemented within the C++ toolkit DEMbox (www.cgp-gateway.org). The movement of each block, governed by the fundamental principle of dynamics, is integrated by means of the velocity-Verlet scheme (Allen and Tildesley [1989]) which is a good compromise between accuracy of the block velocities (for both translations and rotations) and memory saving.

Rock avalanches are far from being treated as a quasi-static evolution of block movements. For this reason, the so-called local non-viscous damping (Cundall et al. [1982]) - which affects the block movements, can not be used since it would lead to unphysical behavior. Indeed, this artefact of calculation dissipates energy in an arbitrary manner. It affects both the kinematics of free bodies and bodies that interact with each other.

Another solution to introduce dissipative behaviour is to account for a local viscous damping at the contact level (Cleary and Prakash [2003]). This

solution has also been set aside because it introduces a viscosity parameter which can not be connected to a well-defined dissipation rate in the case where multiple contacts occur at the same time. More precisely, the effective mass involved in the critical viscosity is not well-defined and should depend on the positions of the contact points and their amount.

In fact, the energy loss may result from very complex physical mechanisms (heat production, wave propagation…) that are beyond our understanding in the case of collective behavior. For the contact-force laws, we wanted a simple formulation while incorporating the energy dissipation due to block impacts. We opted for minimalist laws where friction and normal damping coefficients are required to dissipate the kinetic energy of the blocks. We will see in the sequel that the simple laws proposed here are sufficient to satisfactorily describe the main rebound patterns even if our model is obviously not able to reproduce more complex behaviors like e.g. rocking block (Bourgeot et al. [2006]).

**Block shapes**

In the rock avalanche problematic, the shape of the blocks is of primary importance and it must be taken into account explicitly in the model. Different strategies are possible (e.g. polyhedra, clumps) but we chosed sphero-polyhedra which has several advantages including a highly simplified contact detection (Alonso-Marroquin [2008]). The block shape is defined by a set of vertices interconnected by edges (lines) and faces (Fig. 1). The rounded shape is then defined by sweeping a sphere of radius *r* along each point of its edges and faces. From a mathematical viewpoint, our block shapes can be seen as the Minkowsky sum of a polyhedron with a sphere (Van Den Bergen [2003]).

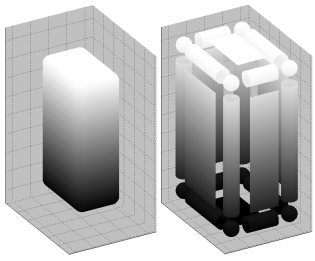

Figure 1. Layout of a brick modelled by sphero-polyhedron.

In practice, the contact position, the overlap and the local frame are determined by considering a few basic geometric computations based on the distances between points, lines and planes. This geometric trick allows the contact area between sphero-polyhedra to be defined by a set of contact points resulting from elementary intersection tests involving the swept sphere radii: (1) vertex-vertex, (2) vertex-edge, (3) edge-edge, and (4) vertex-face. One can better appreciate the benefit of this method when considering for example face-face intersection test: it is simply replaced by a set of edge-edge and vertex-face tests. The sphero-polyhedra method has many other benefits such as the ability to define concave and/or hollow shapes. Also, the normal vectors at contacts are well defined.

**Contact force laws**

The interaction model integrates the energy dissipation related to friction and to normal damping between solids in contact. The most minimalist formulation we found for the normal force is a linear elastic law with two different stiffnesses in case of loading or unloading (Banton et al. [2009]). This way, the rate of non-restored work of the normal force (i.e. the normal restitution parameter $e_n^2$) after an impact is the ratio between the unloading and the loading stiffnesses. As described in Figure 2, the other parameters of the contact law are the Coulomb friction coefficient ($\mu$) and the normal and tangential stiffnesses of the contact ($k_n$ and $k_t$ respectively). The number of parameters of a given contact is therefore equal to four.

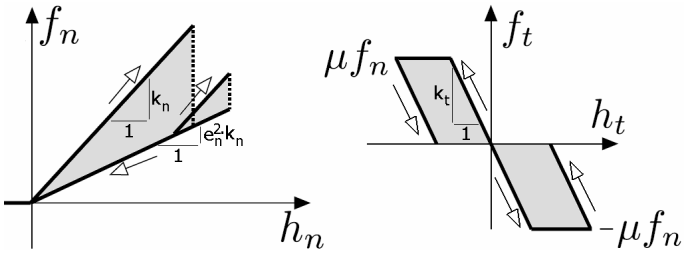


Figure 2. Normal and tangential Force-displacement relations with: $h_n$=normal interpenetration of the two solids, $f_n$=normal repulsive force, $h_t$=tangential relative displacement between the two solids, $f_t$=tangential force. Energy dissipations are represented in grey.

## Assessment of the contact parameters

As an attempt to give the proposed model a predictive character, the physical parameters of the contact law were assessed from additional experiments of the impact of a single brick on a support (clay brick and plastic support called "forex", identical to the ones used by the Manzella and Labiouse [2009]). The brick was filmed at 1,000 images per second by two high-speed cameras positioned along orthogonal directions.

After synchronization (impact time is set as the time origin) and scaling (pixel sizes for each camera), the 2D trajectories of four vertex points for each camera were obtained by means of digital image correlation and made possible the 3D trajectory reconstruction. The parameters involved in the theoretical trajectory (in particular the velocities before and after the impact) were then optimized by means of an error function that gives a distance measure between the identified trajectory and the theoretical one (that obey Newton's second law). Four Brick/Support impacts and two Brick/Brick impacts were analysed, and the contact

parameters were identified for each kind of contact so as to optimize the trajectories of all the studied impacts. The resulting parameters are stored in Table 1. Fig. 3 proposes more visual results, and describes from left to right the different steps of the parameters assessment: (i) experimentation and shooting of the impact, (ii) mathematical identification of the trajectory before and after impact, and (iii) numerical identification of the parameters (stored in Table 1) allowing to optimize the simulation of all the experimental impacts. Figs. 3a and 3b correspond to the two cameras with perpendicular axes used for the shooting.

Table 1. Optimal parameters obtained by minimizing an error function

| | $e_n^2$ | [illegible] | $k_n$ | $k_t/k_n$ |
|---|---|---|---|---|
| Brick/Support | 0.53 | 0.46 | $10^5$ | 0.42 |
| Brick/Brick | 0.13 | 0.86 | $10^5$ | 0.27 |

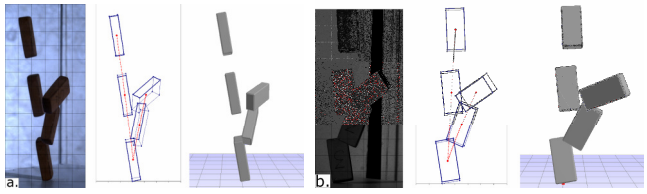


Figure 3. Example of successive steps for the identification of the contacts parameters (time interval of 20ms) ; a. Camera 1 ; b. Camera 2.

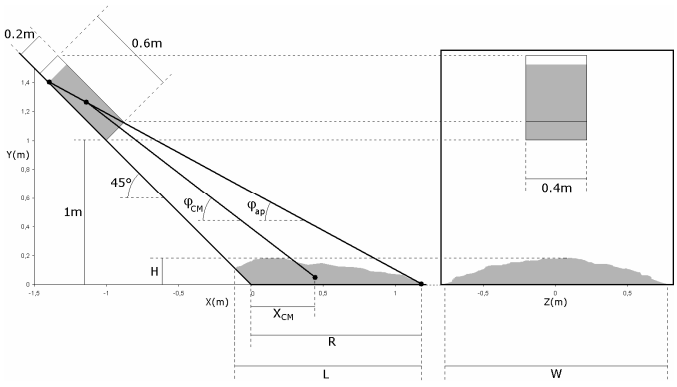


Figure 4. Layout of the experimental device used in Manzella and Labiouse (2009).

## Validation of the model on a small-scale experiment

The contact laws and model parameters have been proved as consistent in the case of a single impact, but a validation is needed to make sure that it is able to predict accurately the behaviour of a granular flow involving a large number of particles. This validation is performed using the experimental results by Manzella and Labiouse (2009). These authors realized a series of launches of a large number of bricks on a device composed by two rectangular boards (3m*4m) of forex (kind of plastic) linked by a hinge. The first board was fixed and horizontal while the second was inclined by a user-defined angle. A rectangular box (height 20cm, width 40cm, depth 60cm) was filled with a given amount of material, and positioned at a determined height on the inclined plane. A trap was open to release the material, which propagated on the slope until it eventually deposited on the horizontal plane. The validation proposed here focuses on one specific experimentation involving 40 litres of randomly poured bricks (size of 3.1cm*1.5cm*0.8cm, material density of 17kN/m$^3$, apparent density of 10kN/m$^3$), launched on a 45° slope from a height of 1m. The bricks and support were identical to the ones used for the identification of the contact parameters in the previous section. The layout of the experiment is represented in Fig. 4, as well as some of the measurements performed on the material deposit : length L, runout R, width W, height H, travel angle $\phi_{CM}$ (related to the centre of mass before and after the flow), and Fahrböschung $\phi_{ap}$ (related to the extremity of the deposit as defined by Heim [1932]).

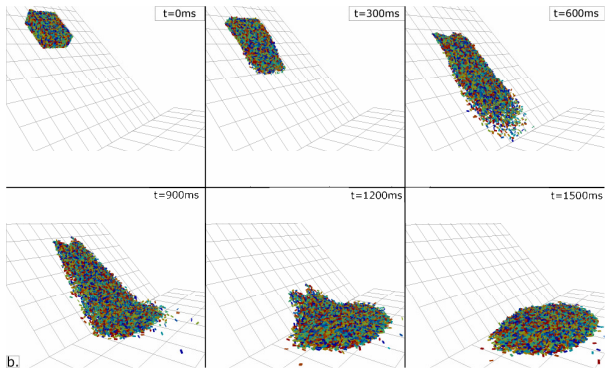


Figure 5. Perspective view of the avalanche predicted by the numerical model.

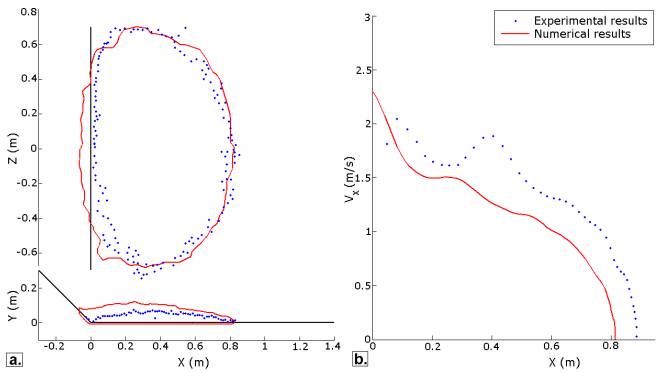


Figure 6. Comparison between the experimental and numerical results; a) horizontal and vertical contours of the deposit; b) Velocity of the avalanche front on the horizontal plane.

This experiment is reproduced numerically with 6300 bricks randomly poured in the starting box. This number of bricks corresponds to a rough estimate of the one used in the actual experiment. The simulation starts when the lower face of the box is deleted. Fig. 5 shows

several stages of the simulated avalanche with a time step of 300ms. The results of the simulation are compared with the experimental ones in Fig. 6. In Fig. 6a, the shapes of the numerical and experimental deposits are compared in terms of their contour in a horizontal and a vertical plane. A very satisfying correspondence appears for the horizontal contour and this correspondence is a bit less accurate for the vertical contour, the numerical deposit having a larger height than the experimental one.

Fig. 6b presents the evolution of the mass front velocity on the horizontal plane with respect to the position of this front, as provided by the experimental and numerical results. The two curves show a good qualitative correspondence. The observed quantitative differences may be linked to the inaccuracy of the concept of "mass front", which has no rigorous and objective definition and was determined by different methods in the experimental and numerical frameworks. Qualitatively, this curve provides some interesting information about the kinematics of the deposit. We first observe a strong reduction of the velocity corresponding to the first impact of the avalanche on the horizontal plane (from x=0m to x=0.2m), then a zone for which the velocity does not decrease a lot, corresponding to the accumulation of the material on the plane (between 0.2m and 0.6m), and finally an important stage of deceleration until the end of the motion (between 0.6m and 0.8m). Table 2 presents a quantitative comparison between the dimensions of the deposit provided by the experiment and by the simulation, and shows a very good correspondence except for the deposit height. This result emphasizes the predictive ability of the proposed numerical model, since this correspondence was achieved by fitting the contact parameters of single-impact experiments instead of running a back-analysis on the full-scale experiment. It shows that it is possible to assess the collective behaviour of a large number of particles if the individual behaviour of each particle is well-defined.

Table 2. Quantitative comparison between the experimental and numerical deposits.

| | L (cm) | R (cm) | W (cm) | H (cm) | $\phi_{CM}$ (°) | $\phi_{ap}$ (°) |
|---|---|---|---|---|---|---|
| Experiment | 93 | 84 | 140 | 7.5 | 40 | 32 |
| Simulation | 88.2 | 82.4 | 138.3 | 12.0 | 40.1 | 32.2 |

## Numerical study of the kinematics of the granular flow

In order to assess the validity of some usual assumptions adopted for continuous modelling of granular flows, the velocity field, angular velocity field, and stress field inside the flow are computed using spatial interpolation techniques. Figure 7 provides in shades of grey the velocity magnitude (in m/s), the angular velocity magnitude (in °/s) of the bricks, and the average stress (in Pa) in the plane of symmetry of the flow, at different stages of the simulation. Figure 7a shows that the velocity magnitude of the particles composing the flow increases regularly while the avalanche develops, and decreases suddenly when the flow reaches the transition between the two planes. The velocity profile in a vertical direction appears to be uniform at any abscise of the flow, and there is no pronounced vertical velocity gradient. It may be seen on Figures 7b and 7c that the magnitudes of the angular velocity of the bricks and of the average stress are much more important around the angle between the two planes than in the slope and in the deposit. It seems therefore that the zone of transition between the two planes induces a brutal reduction of the velocity magnitude, but also triggers an important perturbation of the flow by increasing the rotation of the particles and the stress level. Moreover, the angular velocity of the bricks accumulating on the horizontal plane after the transition is very low, while their velocity is uniform on the deposit and decreases along time until the end of the motion (at t=1.4s). The particles belonging to the accumulated deposit seem therefore to have a slow motion of decelerating translation. This motion is induced by the fact that the particles still falling on the slope transfer their kinetic energy by "pushing" the deposit in the transition zone, inducing the stress peak observed in this area. The displacement of the deposit ends when this transfer of kinetic energy stops, i.e. when there is no more flow on the slope. This assumption is in good agreement with the experimental and numerical estimation of the velocity of the avalanche front (Figure 6).

## Energy considerations

The analysis of the modes of energy dissipation during the flow is a relevant investigation tool to determine the relative importance of each of the parameters of the contact law. Figure 8 depicts the evolution along time of the repartition of the different kinds of energies (potential energy, kinetic energy, dissipated energy) inside the system. At t=0, there is no motion and the system only has potential energy (in white in Figure 8). When the flow develops along the inclined plane (from t=0 to t=0.64s), the part of potential energy decreases and a kinetic energy (shades of grey in the upper part of the figure) appears, due to the velocity of the particles composing the flow. This kinetic energy may be decomposed in its components along the axes x, y, and z, and in rotational energy. Figure 8 shows that only the components along x and y have a significant value, and that the energies along z (lateral spreading of the granular mass) and in rotation are negligible.

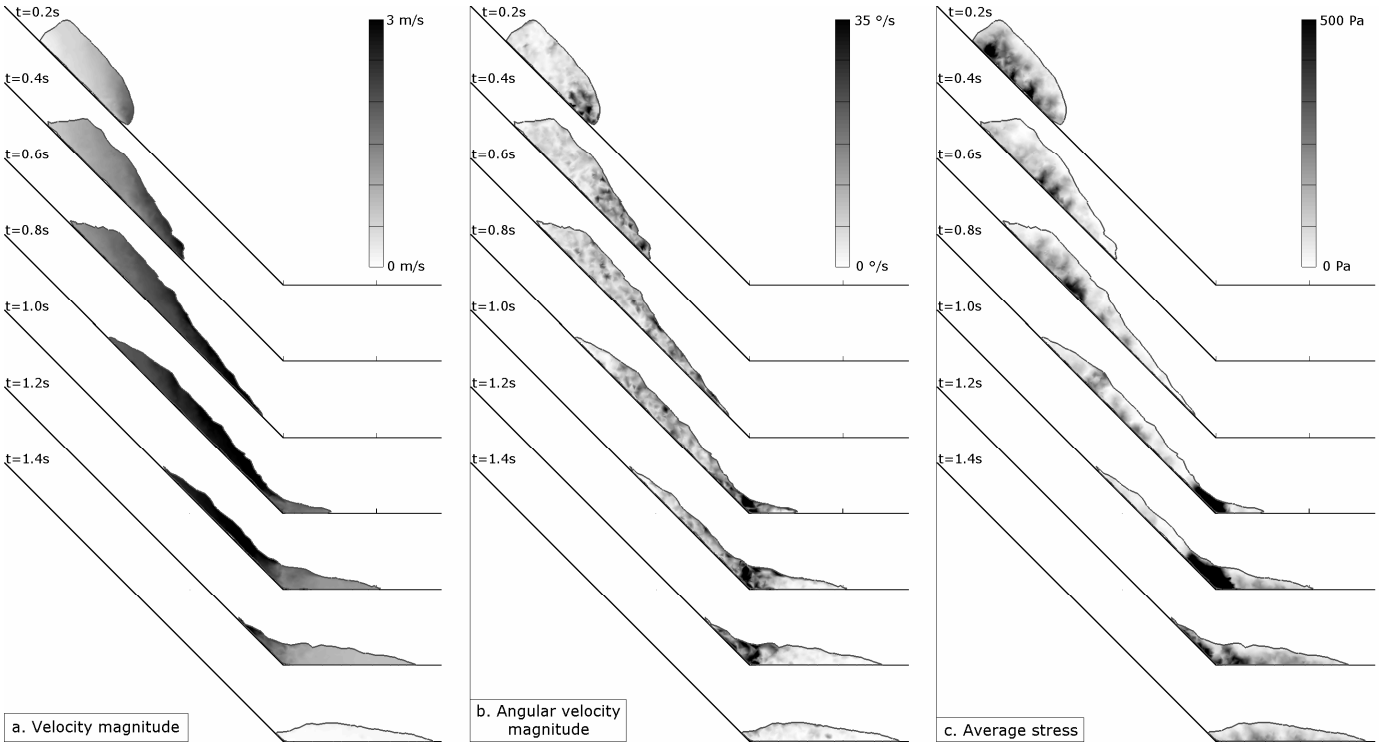


Figure 7. Interpolated fields inside the flow ; a. Velocity magnitude ; b. Angular velocity magnitude ; c. Average stress.

Besides, the sum of the kinetic and potential energies during the flow is not equal to the initial potential energy because of the energy dissipations (shades of grey in the lower part of the figure). These dissipations are related to the contact law depicted in a previous section, and may be decomposed in four categories: Brick-Support frictional dissipation, Brick-Support normal dissipation, Brick-Brick frictional dissipation, and Brick-Brick normal dissipation.

After the impact of the avalanche on the horizontal plane, the kinetic energy reaches a peak and decreases until the end of the motion, at t=1.4s. Meanwhile, there is an increase of the total rate of energy dissipation (i.e. of the slope of the envelope of the total energy dissipation), probably because of the phenomena occurring in the transition zone and pointed out in the previous section. The dissipated energy increases until the motion stops, which corresponds to a dissipation of 100% of the initial potential energy. The proportions of the different kinds of energy dissipations are provided in Figure 8, and clearly show that, over the entire event, most of the energy is dissipated by friction between the support and the bricks (66.2%), and by friction between bricks (24.2%). The dissipations by normal damping are much less significant.

The localizations of the different sources of energy dissipation may be found in Figure 9. To plot this figure, the system was divided in several horizontal slices along the x-axis, each slice having a width of 0.1m. The energy dissipations occurring in each slice were monitored during the simulation, and the figure provides the cumulated dissipated energies of each kind and in each slice during the entire flow.

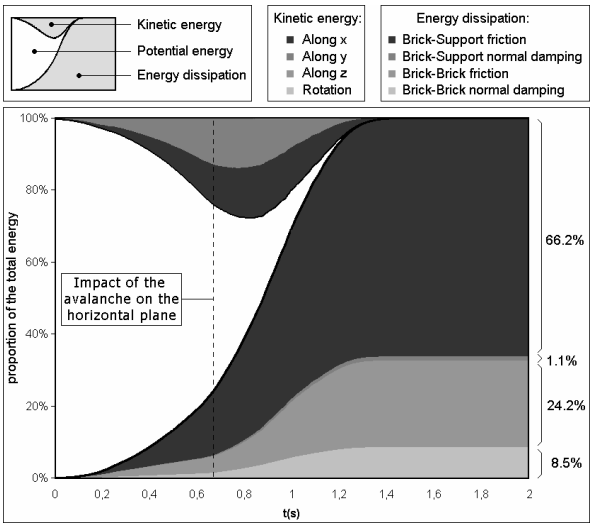


Figure 8. Evolution of the energy repartition inside the system.

In the two planes of the system (i.e. everywhere except in the transition zone around x=0), the figure 9 clearly shows that the energy mostly dissipates by friction between the bricks and the support (around 90% of the total energy dissipated). On the inclined plane, the repartition of this dissipation is roughly uniform, and the dissipation level remains quite low. On the contrary, the transition zone between the two planes exhibits much higher levels and different modes of dissipation. The larger amount of dissipation by contacts between bricks (either by friction or by normal damping) might be related to the phenomena depicted in the previous section (Figure 7), i.e.

to the apparition of important rotations of the particles and to high stress levels because of the flow perturbation induced by the transition between the two planes. This observation probably means that the important proportion of Brick-Support frictional dissipation observed in Figure 8 is only relevant because of the perfect regularity of the slope, and that a granular flow on a slope with important roughness would probably induce a different repartition of the energy dissipations.

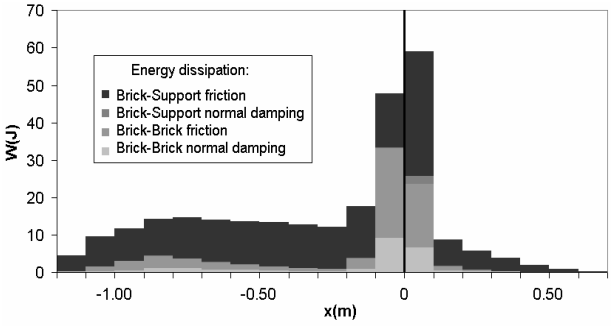


Figure 9. Localisation along the x-axis of the four sources of energy dissipation.

## Conclusion

The mechanisms of propagation of a granular mass were investigated using the discrete element method. The numerical model, calibrated from the elementary rebounds of a single particle, demonstrated the ability to describe accurately the collective movement of a granular flow along a slope. The model was validated from experimental results found in the literature and involving a large number of particles. This model makes possible to assess the position and geometry of the deposit, as well as the kinematics of the whole flow. It also gives access to several quantities (i.e. particle kinematics or energy dissipations) which are out-of-reach of the experimental devices. It was for example demonstrated that, along the slope, most of the energy is dissipated by basal friction between the bricks and the support. The velocity field being rather homogeneous, it induces a small number and intensity of the impacts inside the flow, which leads to a limited dissipation related to these impacts in this zone of the flow. On the contrary, the slope transition constitutes an obstacle to the flow which is therefore strongly perturbed. The contacts between bricks are much more numerous and intense, which leads to the apparition of energy dissipations by friction and normal damping between bricks. The downstream part of the flow (located on the horizontal plane) is slowed down by the absence of slope, and its motion is only triggered by the transfer of kinetic energy from the upstream part of the flow. For the complete event, the proportions of the different modes of energy dissipation are 66.2% by Brick-Support friction, 24.2% by Brick-Brick friction, and respectively 8.5% and 1.1% by Brick-Brick and Brick-Support normal damping.

The proposed model was applied to laboratory experiments with simple and controlled geometric parameters, and must be confronted to more complicated topographies and block shapes. It is likely that a lack of regularity of the slope may considerably change the characteristics of the flow. The procedure of determination of the model parameters, which proved relevant for laboratory tests, has also to be tested on in-situ block impacts. Only when this procedure is validated will it be possible to obtain predictive results for real granular flow events such as rock avalanches.

## Acknowledgments

This study was performed as a part of the European project ALCOTRA-MASSA, with financial support from the European Funds For Regional Development (FEDER).

## References

M. P. Allen and D. J. Tildesley. Computer simulation of liquids. Clarendon Press, New York, NY, USA, 1989.

F. Alonso-Marroquin. Spheropolygons: A new method to simulate conservative and dissipative interactions between 2d complex-shaped rigid bodies. EPL (Europhysics Letters), 83(1):14001, 2008.

J. Banton, P. Villard, D. Jongmans, and Scavia C. Two-dimensional discrete element models of debris avalanches: parameterisation and the reproducibility of experimental results. Journal of Geophysical Research Earth Surface, 114, 2009.

J.-M. Bourgeot, C. Canudas-de Wit, and B. Brogliato. Rocking block to the biped robot impact shaping for double support walk: From the. In M.O. Tokhi, G.S. Virk, and M.A. Hossain, editors, Climbing and Walking Robots, pages 509-516. Springer Berlin Heidelberg, 2006.

P.W. Cleary and M. Prakash. Discrete-element modelling and smoothed particle hydrodynamics: potential in the environmental sciences. Philosophical Transactions of the Royal Society A: Mathematical, Physical and Engineering Sciences, 362:2003.

P.A. Cundall and O.D.L. Strack. A discrete numerical-model for granular assemblies. Geotechnique, 29(1): pp. 47-65, 1979.

P.A. Cundall, A. Dresher, O.D.L. Strack, in *IUTAM Conference on Deformation and Failure of Granular Materials* (Delft, The Netherlands, 1982)

A. Heim, *Bergsturz und Menschenleben*, 218 pp., Fretz und Wasmuth Verlag, Zürich, 1932.

A. Mangeney-Castelnau, J.P. Vilotte, M.O. Bristeau, B. Perthame, F. Bouchut, C. Simeoni, and S. Yerneni. Numerical modeling of avalanches based on saint venant equations using a kinetic scheme. J. Geophys. Res.-Solid Earth, 108, 2003.

I. Manzella and V. Labiouse. Flow experiments with gravel and blocks at small scale to investigate parameters and mechanisms involved in rock avalanches. Engineering Geology, 109, 2009.

S. McDougall and O. Hungr. A model for the analysis of rapid landslide motion across three-dimensional terrain. Can. Geotech. J., 41:1084 -1097, 2004.

P. Tommasi, P. Campedel, C. Consorti, and R. Ribacchi. A discontinuous approach to the numerical modelling of rock avalanches. Rock Mech. Rock Engng, 41(1): pp. 37-58, 2008.

G. Van Den Bergen. Collision Detection in Interactive 3D Environments (The Morgan Kaufmann Series in Interactive 3D Technology). Morgan Kaufmann, October 2003.